Volume 1 | Number 1 | Jan 2013 | Pages 1–100

Journal of
Materials Chemistry A

Materials for energy and sustainability
www.rsc.org/materialsA

ROYAL SOCIETY OF CHEMISTRY

ROYAL SOCIETY OF CHEMISTRY

www.rsc.org/materialsA

ARTICLE TYPE

PTC MWCNTs/DI-water Switchable composites

Pengcheng Sun,[a,b] Yun Huang,[b] Jun Yang,[b] Guoan Cheng,[a] and Ruiting Zheng[*a]

5 **Switchable electrical and thermal conductivities are desirable in many applications such as automatic regulation of building temperature, circuit protection, etc. In this paper, we study the electrical and thermal conductivities of multi-walled carbon nanotubes(MWCNTs)/ DI-water composites via first** 10 **order phase transition. We demonstrate that, with SDBS functionalized MWCNTs, the composites show unique positive temperature coefficient (PTC) electrical switching and negative temperature coefficient (NTC) thermal switching properties. Around the 0 °C, the corresponding** 15 **contrast ratio of electrical and thermal conductivities reaches 1250 and 3.58 times respectively.**

Introduction

Brine rejection is a very interesting natural phenomenon in the course of salt solution freezing, which is caused by the big 20 difference of salt solubility between liquid water and ice[1]. Brine rejection has obvious influences on the mechanical, biological and transport properties of the solution system[2,3]. One of the famous instances is the critical permeability phenomenon of sea ice[4]. Inspired by the rejection effects, transport properties of 25 freezable suspensions are studied recently. By dispersing graphite flakes, MWCNTs and SWCNTs into hexadecane and octadecane, electrical and thermal conductivity switchable composites are achieved[5-8]. During the freezing, the conductive nanoparticles are squeezed to the grain boundary of the organic crystals. 30 Percolation networks and stress-generation during crystallization reduces the electrical and thermal contact resistances in composites, leading to large changes in the electrical and/or thermal conductivities. The contrast ratio of electrical conductivity (EC) and thermal conductivity(TC) of the switching 35 composites reached 5 orders and 3.2 times respectively[6,7]. The reversible tuning of suspensions' electrical and thermal properties near room temperature by first-order phase transition opens a door for developing new thermosensitive materials with flexible critical temperatures, and also sparks the transport mechanism 40 researches of phase transition composites[9-11].

So far, most of organic fluids based composites show NTC effects; PTC effects are not reported. In this paper, the electrical and thermal properties of MWCNTs/deionized(DI) water 45 composites were studied. We find that, for the first time, the EC of the sodium dodecyl benzene sulfonate(SDBS) functionalized MWCNTs (S-MWCNTs) aqueous suspensions shows unique

PTC effect, but the TC of which still shows NTC effect. The biggest EC and TC contrast around the water-ice transition point 50 are 3 orders and 3.58 times respectively. The mechanism of PTC effect in the S-MWCNTs aqueous suspensions is investigated too.

Results and discussion

55 In this paper, we use high purity (>95％) short MWCNTs to fabricate the composites. Figure1a is the SEM image of raw MWCNTs(R-MWCNTs), which are uniformly dispersed on the Si substrate. The length of the R-MWCNTs is about 0.5－1 um and the diameter is about 10–15 nm. High-resolution 60 transmission electron microscopy (HRTEM) image indicate that the R-MWCNT has well defined multi-layered structure and smooth surface (Figure 1b). After the 2 hours of acid treatment, several external layers of the R-MWCNT are damaged under the attacking of the oxidative groups, but the structure of internal 65 layers are well kept (Figure 1c)[12]. In contrast, the HRTEM image of the S-MWCNT shows a layer of amorphous structure attached on the surface of MWCNT. The thickness of the amorphous layer is about 1nm(Figure 1d), which may comes from the absorption of the SDBS[13]. Figure 1e shows the Fourier Transform IR (FTIR) 70 spectrum of R-MWCNTs, O-MWCNTs and S-MWCNTs, respectively. For R-MWCNTs, the peak at 1632 cm^{-1} corresponds to the C=C stretching mode of the graphite structure[14]. The peaks at 1384 cm^{-1} and 3432 cm^{-1} come from the C-H bending mode and O-H stretching mode respectively[15], which may caused by 75 the surface adsorption of hydrocarbon and water contamination[14,15]. After oxidative treatment, additional peaks at 1706 cm^{-1} and 1200 cm^{-1} appeared on the O-MWCNT samples, which may due to the stretching mode of C=O and C-O. For S-MWCNT samples, the peaks at 2916 cm^{-1}, 2848 cm^{-1} and 1443 cm^{-1} are come from 80 the C-H stretching modes and bending modes of the SDBS. The peak around 1170 cm^{-1} should be caused by S-O mode[16,17]. The FTIR results confirm the O-MWCNTs and S-MWCNTs are covered by the oxidative groups and SDBS respectively.
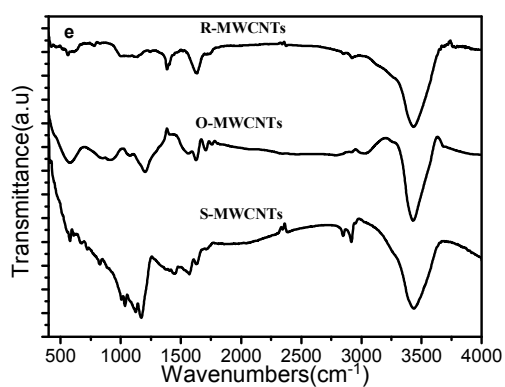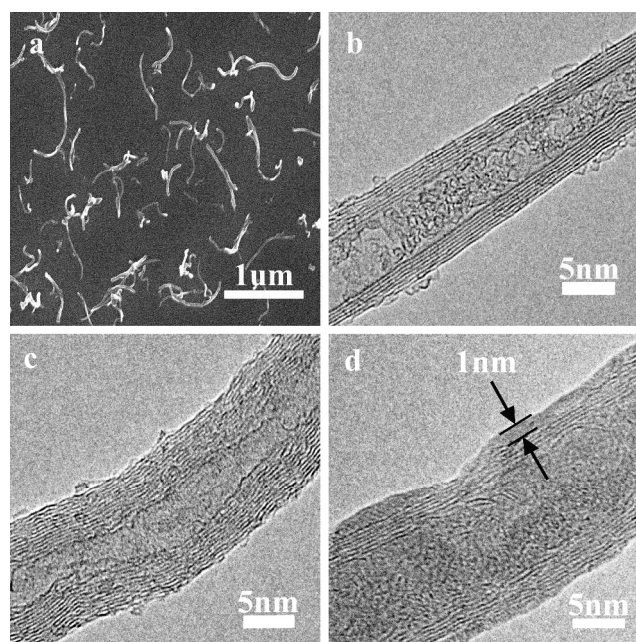
Fig.1 (a) SEM image of the R-MWCNTs dispersed on the silicon
5 substrate. (b-d) HRTEM images of the R-MWCNT, O-MWCNT and S-MWCNT respectively. (e) Mid-IR spectrum of the MWCNTs after different functionalization.

Dispersion of MWCNTs in aqueous media has been substantially
10 studied in previous research[13, 18, 19], surface functionalization is found to be effective ways for getting stable MWCNTs suspensions[20]. However, the re-dispersion property of nano-materials in water has been barely concerned, which is very important for the phase transition nano-composites. In this paper,
15 the microstructure of the dilute O-MWCNTs and S-MWCNTs DI-water composites(0.05% volume fraction) during the phase change is observed by an optical microscope, as shown in figure 2. In the liquid state, the distribution of O-MWCNTs in DI-water is relatively uniform. The size of most O-MWCNTs clusters are
20 several micrometers, a minority of big clusters tends to be tens of microns (Figure.2 a). The optical photo of 0.2%V/V O-MWNTs/DI-water suspensions are shown in the insert picture of Figure 2a, no phase separation is observed after one month of standing, which shows a good stability of the samples. The

25 corresponding Zeta potential of O-MWNTs is measured to be -51.5mV. After three times of frozen and molten, the O-MWCNTs tend to agglomerate by the repeated squeeze of the ice crystals, the size of the clusters grows to about 100 microns (Figure 2b). Obvious phase separation happens in the corresponding
30 suspensions because of the settlement of the big O-MWNTs clusters (insert picture of Figure 2b). In comparison, the S-MWCNTs show better dispersion in DI-water (Figure 2c), the cluster size of S-MWCNTs is about several microns, few big clusters are observed. There is also no phase separation in the
35 suspension after one month of standing (insert picture of Figure 2c) too, the corresponding Zeta potential of S-MWCNT is -60mV. After three times of re-melting, majority of the S-MWCNT clusters are still well separated, only a few S-MWCNT clusters grow to 10-20 microns (Figure 2d). The 0.2%V/V S-
40 MWCNTs/DI-water suspension shows no phase separation after three times of re-freezing (insert picture of Figure 2d), which indicates a better re-dispersion property of S-MWCNTs/DI-water suspensions than that of O-MWCNTs/DI-water suspensions.
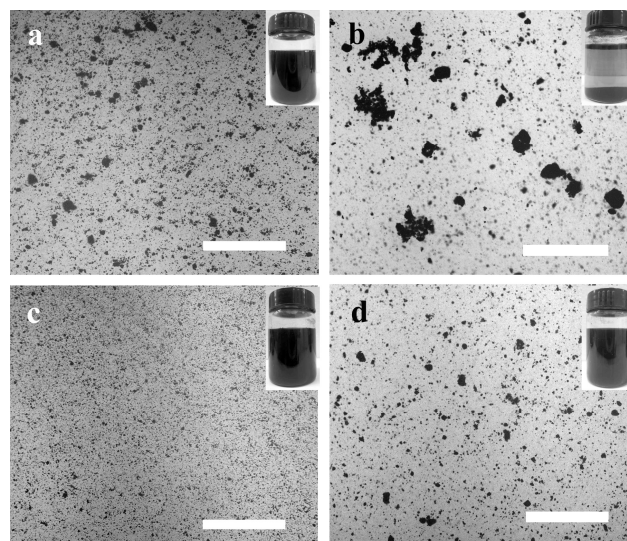

Fig.2 Evolution of MWCNTs microstructures in DI-water during the remelting process. a,b) Images of 0.05%(V/V) O-MWCNTs/DI-water composites in original liquid state, after three times re-melting, respectively. c,d) Images of 0.05%(V/V) S-MWCNTs/DI-water
50 composites in original liquid state, after three times re-melting, respectively. The insert pictures are the digital photos of the corresponding suspensions. Scale bars in a-d are all corresponding to 200 μm.

55 The different re-dispersion behaviors of the MWCNTs should attribute to their different surface properties. As we know, O-MWCNTs stabilized in DI-water by the electrostatic repulsion effects of the negative electric charged oxidative groups[19]. Using SDBS as surfactant, both electrostatic repulsion and steric
60 repulsion that caused by longer alkyl chain work during the dispersion process[13]. When the composite is freezing, the MWCNTs trend to be squeezed together under the strong pressure, which is much bigger than the corresponding repulsion force. As the ice crystal melts, the electrostatic repulsion force is
65 insufficient to totally separate the MWCNTs. However, the steric

effect of SDBS could push the S-MWCNTs away from each other, which is crucial for the good re-dispersion properties of MWCNTs/DI-water composites. The similar re-dispersion mechanism is also found in the octadecylamine (ODA) functionalized MWCNTs/hexadecane composite[6].

The electrical and thermal transport properties of the S-MWCNTs/DI-water composites around the phase transition point are shown in Figure3. In the liquid state, the EC of the composites varies a little with the change of temperature (Figure 3a). From -0.5 to 0.5 $^\circ$C, the EC increases several orders. After the DI-water is completely frozen, the EC stabilizes. In the liquid state, The EC increases from 4.4×10^{-2}S m^{-1} to 2.2×10^{-1}S m^{-1} with the S-MWCNT loading increase from 0.2% to 1%(5℃). In the solid state, the corresponding EC also changes from 6.9×10^{-5}S m^{-1}(0.2%) to 3.7×10^{-4}S m^{-1}(1%)(-5℃). The biggest EC contrast ratio between -5℃ and 5℃ is 1250 times at the volume fraction of 0.8%. TC of the S-MWCNTs/DI-water composites as a function of temperature is shown in Figure 3b. TC of the liquid composite changes little with the increase of temperature. In the course of freezing, the TC increases sharply. After the composite is completely frozen, the TC stabilizes too. For the S-MWCNTs/DI-water composites, in both solid and liquid states, the TC of composites enhances with the increase of the S-MWCNT loading. The TC contrast ratio peaks 3.58 times at the volume fraction of 0.4%(V/V). The corresponding TC changes from 0.677W/mK (liquid) to 2.43W/mK (solid) as the temperature decreases from 5℃ to -5℃.
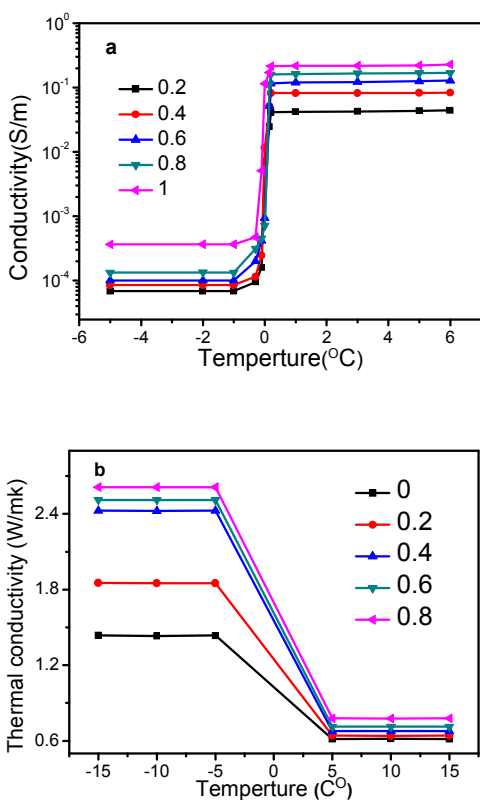
fractions. (b) TC of the MWCNTs/DI-water composites with different CNTs volume fractions.

The EC of the S-MWCNTs/DI-water composites is higher in the liquid state, but lower in the solid state, which is contrary to hexadecane based composites[6, 7]. As an efficient transport paths, MWCNTs could improve the transport properties of the composites in both liquid and solid state, but the distinct improvement will only happens when the MWCNTs percolation structures formed in the solid state[21]. That's why most oil based composites show NTC EC effect. We conjecture that the SDBS plays an important role for the PTC EC switching properties of S-MWCNTs/DI-water composites. Figure 4 is the schematic diagram of the phase transition process in S-MWCNTs/DI-water composite. In the liquid composite, SDBS is ionized into $C_{18}H_{29}SO_3^{-1}$ and Na^{+1} in DI-water. Alkyl chains with SO_3^{-1} group will attach on surface of S-MWCNTs, the electrostatic repulsion and steric effect of the surfactant prevent the formation of S-MWCNTs transport networks, which makes S-MWCNTs contribute less to EC (Figure 4a). However, as an effective carrier, a large quantity of Na^{+1} ions should enhance the EC effectively in the liquid composites[22]. As shown in Figure 4b, when the liquid composites change into solids, the Na^{+1} ions trend to migrate to the grain boundary of the ice crystals[4, 23]. The electrical conductivity of the solid composites mainly comes from the S-MWCNTs transport networks. The PTC effect in S-MWCNTs/DI-water composites may due to the EC comes from the Na^{+1} transfer in liquid water is much bigger than the electron transport within S-MWCNTs networks in the solid composites.

Fig.3 Variation of EC and TC around the phase transition point. (a) EC of the MWCNTs/DI-water composites with different CNTs volume
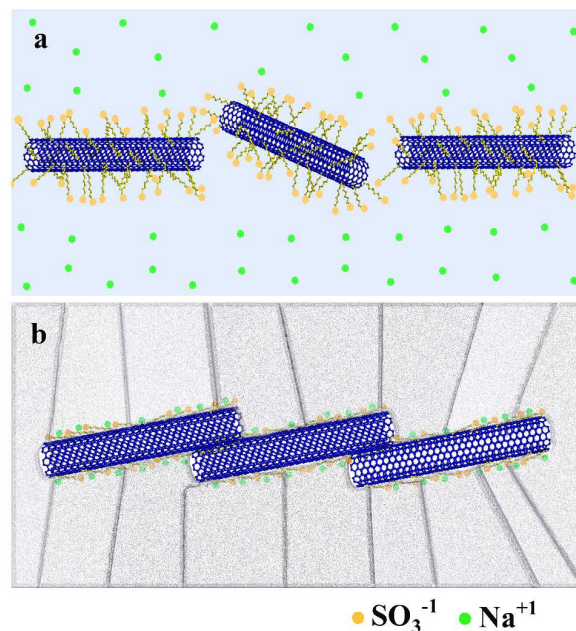

Fig.4 Schematic diagram of the phase transition process in S-MWCNTs composite. a) Liquid state, S-MWCNTs are well dispersed by the help of surface functional groups. b) Frozen state, S-MWCNTs are squeezed to the grain boundary and form a transport network.

EC of the liquid composites can be calculated by considering the molar conductivity and concentration of Na^{+1}. The EC of

electrolyte solution can be expressed as k=Λ_mc, in which k, Λ_m and c are the EC, molar conductivity and ion concentration of the solution, respectively. As the volume fraction of S-MWCNTs raises from 0.2％ to 1％, the Na^{+1} concentration in liquid composites increases from 0.0241mol/L to 0.121mol/L. According to the report of Barthel et.al[24], the molar conductivities of Na^{+1} in water at 5℃ are about 30.31×10^{-4} and 30.27×10^{-4}S m^2 mol^{-1} respectively at the concentration of 0.0241 and 0.121mol/L. The calculated EC of the liquid composites increase from 0.073 S m^{-1}(0.2％) to 0.366 S m^{-1}(1％). The EC of the liquid composites in our experiment changes from 0.044 S m^{-1}(0.2％) to 0.22 S m^{-1}(1％) at the 5℃. The theoretical and measured EC values of are of the same order, which confirms the EC of the liquid composites is mainly contributed by Na^{+1} transport. The difference of the EC values may due to the S-MWCNT's block for Na^{+1} transport. In the solid composites, as the volume fraction of the S-MWCNTs increases from 0.2% to 0.8％(V/V), the transport networks are improved, which should be responsible for the increasing EC in the solid composites. The substantially enhancement of the EC from 0.8-1％(V/V) may be caused by the formation of the complete networks in the high concentrations[25]. We think the SDBS surfactant plays a vital role for the low EC of the solid composites. First, the π-π stacking of SDBS leads to disturbances of the π-electrons delocalization of the S-MWCNTs surfaces, which results in a significant deterioration of electrical properties of S-MWCNTs[18]. In another way, the amorphous SDBS coated on the surface of S-MWCNTs could cause the tremendous contact resistance between S-MWCNTs[26, 27], which further cause a obvious decrease of EC in S-MWCNTs network. Thus, the unique PTC EC property of the S-MWCNTs/DI-water composites is dominated by the transport mechanism of Na^{+1} in the liquid and solid composites respectively.

The largest TC contrast ratio of S-MWCNTs/DI-water composites is 3.58 times between -5℃ and 5℃, but the TC contrast ratio between pure DI-water and ice is only about 2.33times. The migration of Na^{+1} contribute little to the thermal transport in liquid composites[28]. The TC enhancement in the solid state should attribute to that phonon transport faster along the S-MWCNTs networks[29]. That is why TC still shows NTC effect. From 0.2％-0.4％(V/V), the TC of the solid composites enhance a lot, we anticipate that the big enhancement is also due to the formation of S-MWCNTs percolation networks. As we further increase the S-MWCNTs volume fraction, the TC turns to be saturate.

The durability of the S-MWCNTs/DI-water composites is evaluated by testing the cycling properties of the composites. The EC cycling property of the 0.8%(V/V) S-MWCNTs/DI-water composites is shown in Figure 5a. In the first three cycles, the EC increases from 9.56×10^{-5}S/m to 1.34×10^{-4}S/m in the solid state and varies from 1.18×10^{-1} S/m to 1.67×10^{-1} S/m in the liquid state. The corresponding EC contrast ratio changes from 1234 to 1250 times. After three times recycle, the ratio of the EC becomes stable and approaches a constant(3 orders of magnitude). The TC cycling property of 0.4％ (V/V) S-MWCNTs/DI-water composites is shown in Figure 5b. In first

three cycles, TC increases from 0.615 W/mK to 0.677 W/mK in the liquid state, but decreases from 2.67 W/mK to 2.43 W/mK in the solid state, the corresponding TC contrast ratio decreases from 4.34 to 3.58 times. After the first three cycles, the TC turns to stable in both the liquid and the solid state, and the TC contrast ratio stabilizes at about 3.58 times.
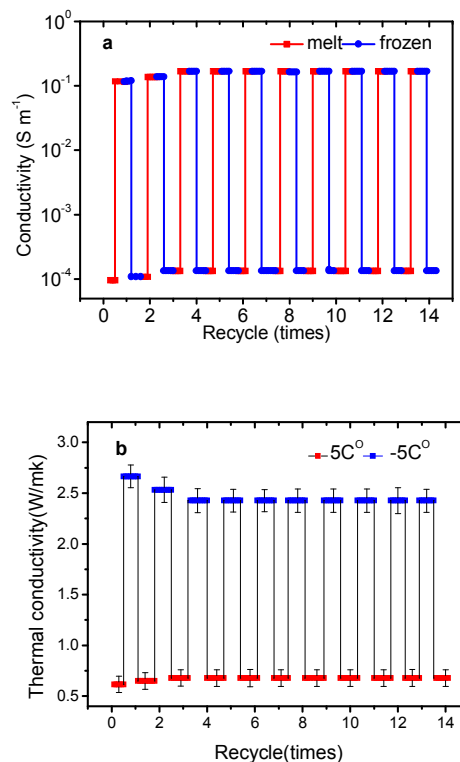

Fig.5 Repetitive behavior tests of the S-MWCNTs/DI-water composites. (a)EC. (b)TC.

The variation of EC and TC contrast ratio is thought to be closely related to the microstructure evolution of S-MWCNTs composites during the freezing/remelting cycles. The growth of the S-MWCNTs clusters in the re-melting process should be responsible for the change of EC and TC contrast ratio in the first three cycles. The growth of S-MWCNTs clusters will be beneficial to the enhancement of EC in both liquid and solid composites, because the bigger clusters have higher efficiency for electron transport[21, 25]. And the effective aggregate of S-MWCNTs is also helpful for TC increment in the liquid composites[30]. But the worse dispersion of S-MWCNTs will decrease TC in the solid composites, as other researchers also observed[31, 32]. After the variation of the first three cycles, the structure of S-MWCNTs cluster is stabilized, the EC and TC contrast ratio stabilize too.

Conclusions

In conclusion, switchable EC and TC transport properties of MWCNTs/DI-water composites caused by phase transition are studied. The re-dispersion and transport properties of the composites are regulated by the surface functionalization of MWCNTs. By using SDBS functionalized MWCNTs, the biggest EC and TC contrast ratio of 3 orders and 3.58 times nearby the

freezing point are achieved. The S-MWCNTs/DI-water composites show unique PTC EC and NTC TC property. The DI-water based switching composite shows high temperature coefficient, low cost and good durability, which have great potential in sensors, smart control, thermal storage and other related area.

Acknowledgements

Notes and references

[a]Key Laboratory of Radiation Beam Technology and Materials Modification of Ministry of Education, College of Nuclear Science and Technology, Beijing Normal University, Beijing 100875, P. R. China. Email: rtzheng@bnu.edu.cn
[b]State Key Laboratory of Multi-phase Complex Systems, Institute of Process Engineering, Chinese Academy of Sciences, Beijing 100190, China.
† Electronic Supplementary Information (ESI) available: Descriptions of experimental methods and additional information. See DOI: 10.1039/b000000x/

1. L. Vrbka and P. Jungwirth, *Physical review letters*, 2005, **95**, 148501.
2. A. Y. Shcherbina, L. D. Talley and D. L. Rudnick, *Science*, 2003, **302**, 1952-1955.
3. K. Caldeira and P. B. Duffy, *Science*, 2000, **287**, 620-622.
4. K. M. Golden, S. F. Ackley and V. I. Lytle, *Science*, 1998, **282**, 2238-2241.
5. T. Zhang and T. Luo, *ACS Nano*, 2013, **7**, 7592-7600.
6. P. Sun, Y. Wu, J. Gao, G. Cheng, G. Chen and R. Zheng, *Advanced Materials*, 2013, **25**, 4938-4943.
7. R. Zheng, J. Gao, J. Wang and G. Chen, *Nature Communications*, 2011, **2**, 289.
8. S. Harish, K. Ishikawa, S. Chiashi, J. Shiomi and S. Maruyama, *The Journal of Physical Chemistry C*, 2013, **117**, 15409-15413.
9. J. W. Gao, R. T. Zheng, H. Ohtani, D. S. Zhu and G. Chen, *Nano Letters*, 2009, **9**, 4128-4132.
10. Z. Liu, R. Zou, Z. Lin, X. Gui, R. Chen, J. Lin, Y. Shang and A. Cao, *Nano letters*, 2013, **13**, 4028-4035.
11. B. Wang, J. Hao, Q. Li and H. Li, *International Journal of Thermal Sciences*, 2014, **83**, 89-95.
12. V. Datsyuk, M. Kalyva, K. Papagelis, J. Parthenios, D. Tasis, A. Siokou, I. Kallitsis and C. Galiotis, *Carbon*, 2008, **46**, 833-840.
13. M. F. Islam, E. Rojas, D. M. Bergey, A. T. Johnson and A. G. Yodh, *Nano Letters*, 2003, **3**, 269-273.
14. U. J. Kim, C. A. Furtado, X. Liu, G. Chen and P. C. Eklund, *Journal of the American Chemical Society*, 2005, **127**, 15437-15445.
15. E. Fuente, J. Menendez, M. Diez, D. Suarez and M. Montes-Moran, *The Journal of Physical Chemistry B*, 2003, **107**, 6350-6359.
16. B. R. Priya and H. J. Byrne, *The Journal of Physical Chemistry C*, 2007, **112**, 332-337.
17. Z. P. Xu and P. S. Braterman, *Journal of Materials Chemistry*, 2003, **13**, 268-273.
18. E. E. Tkalya, M. Ghislandi, G. de With and C. E. Koning, *Current Opinion in Colloid & Interface Science*, 2012, **17**, 225-232.
19. L. Jiang, L. Gao and J. Sun, *Journal of Colloid and Interface Science*, 2003, **260**, 89-94.
20. H. Xie and L. Chen, *Journal of Chemical & Engineering Data*, 2011, **56**, 1030-1041.
21. J. Li, P. C. Ma, W. S. Chow, C. K. To, B. Z. Tang and J. K. Kim, *Advanced Functional Materials*, 2007, **17**, 3207-3215.
22. G. Eisenman, *Analytical Chemistry*, 1968, **40**, 310-320.
23. J. H. Kim, T. Shin, K. H. Jung and H. Kang, *ChemPhysChem*, 2005, **6**, 440-444.
24. M. Bešter-Rogač, R. Neueder and J. Barthel, *Journal of solution chemistry*, 1999, **28**, 1071-1086.
25. W. Bauhofer and J. Z. Kovacs, *Composites Science and Technology*, 2009, **69**, 1486-1498.
26. C. Li, E. T. Thostenson and T.-W. Chou, *Applied Physics Letters*, 2007, **91**, -.
27. F. H. Gojny, M. H. G. Wichmann, B. Fiedler, I. A. Kinloch, W. Bauhofer, A. H. Windle and K. Schulte, *Polymer*, 2006, **47**, 2036-2045.
28. J. Eapen, J. Li and S. Yip, *Physical review letters*, 2007, **98**, 028302.
29. R. Zheng, J. Gao, J. Wang, S.-P. Feng, H. Ohtani, J. Wang and G. Chen, *Nano Letters*, 2011, **12**, 188-192.
30. R. Prasher, P. E. Phelan and P. Bhattacharya, *Nano Letters*, 2006, **6**, 1529-1534.
31. S. H. Song, K. H. Park, B. H. Kim, Y. W. Choi, G. H. Jun, D. J. Lee, B.-S. Kong, K.-W. Paik and S. Jeon, *Advanced Materials*, 2013, **25**, 732-737.
32. J. E. Peters, D. V. Papavassiliou and B. P. Grady, *Macromolecules*, 2008, **41**, 7274-7277.

Graphical abstract. Switchable electrical and thermal conductivities are desirable in many applications such as automatic regulation of building temperature, circuit protection, etc. In this paper, we study the electrical and thermal conductivities of multi-walled carbon nanotubes(MWCNTs)/ DI-water composites via first order phase transition. We demonstrate that, with SDBS functionalized MWCNTs, the composites show unique positive temperature coefficient (PTC) electrical switching and negative temperature coefficient (NTC) thermal switching properties. Around the 0 ºC, the corresponding contrast ratio of electrical and thermal conductivities reaches 1250 and 3.58 times respectively.